iScience

CellPress
OPEN ACCESS

Article

Wearable strain sensor for real-time sweat volume monitoring

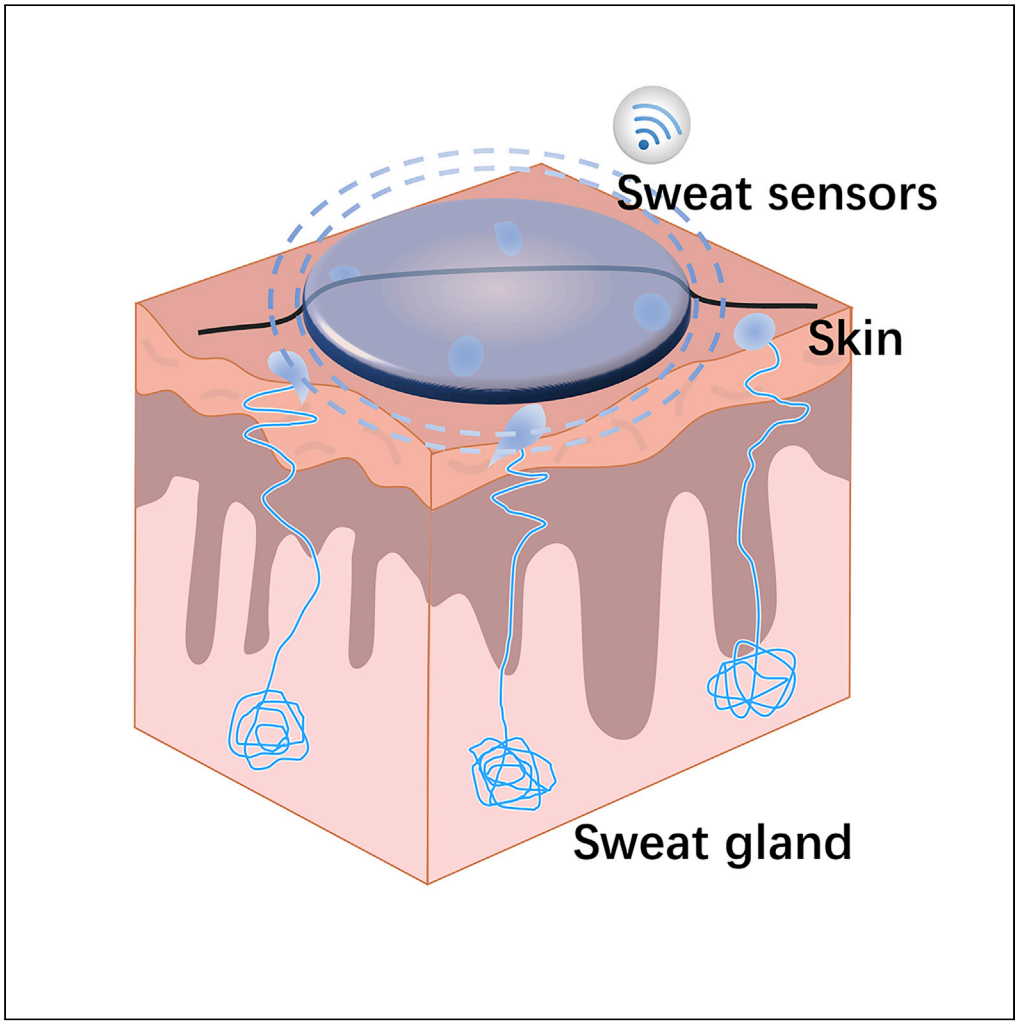

Lirong Wang, Tailin Xu, Chuan Fan, Xueji Zhang

xutailin@ustb.edu.cn (T.X.)
zhangxueji@ustb.edu.cn (X.Z.)

HIGHLIGHTS

A wearable strain sensor for real-time sweat volume monitoring is firstly reported

Such sensor converts sweat volume into intuitive changes in the resistivity

The sensor shows excellent repeatability, stability, and reliability

Wang et al., iScience 24, 102028
January 22, 2021
https://doi.org/10.1016/j.isci.2020.102028

iScience

CellPress
OPEN ACCESS

Article

Wearable strain sensor for real-time sweat volume monitoring

Lirong Wang,[1] Tailin Xu,[1,2,3,*] Chuan Fan,[1] and Xueji Zhang[1,2,*]

SUMMARY

Reliably monitoring sweat volume has attracted much attention due to its important role in the assessment of physiological health conditions and the prevention of dehydration. Here, we present the first example of wearable strain sensor for real-time sweat volume monitoring. Such sweat volume monitoring sensor is simply fabricated via embedding strain sensing fabric in super-absorbent hydrogels, the hydrogels can wick sweat up off the skin surface to swell and then trigger the strain sensing fabrics response. This sensor can realize real-time detection of sweat volume (0.15–700 μL), shows excellent repeatability and stability against movement or light interference, reliability in the non-pathological range (pH: 4–9 and salinity: 0–100 mM NaCl) in addition. Such sensor combing swellable hydrogels with strain sensing fabrics provides a novel measurement method of wearable devices for sweat volume monitoring.

INTRODUCTION

Sweat is an attractive biofluid for wearable biosensors owing to its relatively easy collection without an invasive procedure, as well as containing a heterogeneous blend of biomarkers related to health condition (Bandodkar et al., 2019b; Bariya et al., 2018; Brothers et al., 2019; Choi et al., 2018; Gao et al., 2016; Kim et al., 2019; Koh et al., 2016; Ray et al., 2019; Wang et al., 2017; Yang and Gao, 2019; Yang et al., 2019). Sweat sensors are closely related to sweat volume and rate, which is extremely important for accurate detection of sweat biomarkers (He et al., 2019, 2020; Heikenfeld, 2016; Kaya et al., 2019; Liu et al., 2020; Sonner et al., 2015). Traditionally, the methods for sweat volume and rate measurements are based on body mass change and sweat patch analysis, which always requires professional workers and specialized laboratories (Baker et al., 2011). Recently, conductometric, colorimetric, and volumetric analysis sensing methods have been developed, providing new technologies for wearable sweat sensors to detect sweat volume and rate (Bandodkar et al., 2019a; Francis et al., 2018; Kim et al., 2018; Koh et al., 2016; Nyein et al., 2018, 2019; Yuan et al., 2019; Zhao et al., 2019a). Nevertheless, most of the above approaches are difficult to directly obtain the accurate readings. More direct and accurate detection approaches are highly required to fulfill the demanding detection requirements.

Strain sensors as an important subfield of wearable electrics, which can translate mechanical deformations (stretching, compression, bending, twisting, etc.) into the recordable changes of sensor element property (Kim et al., 2017; Park et al., 2014; Tee1 et al., 2015; Tian et al., 2020; Zhang et al., 2017a; Zhang et al., 2017b), are showing promising applications in electronic skin (Hua et al., 2018), personalized health monitoring (Kang et al., 2014, 2019; Trung and Lee, 2016; Yang et al., 2020), prosthesis (Kim et al., 2014; Tee1 et al., 2015), human-machine interaction (Lim et al., 2015; Liu et al., 2017), and soft robotics (Hines et al., 2017). Compared with traditional electronic devices, wearable strain sensors have many unique properties to adapt to human activities, such as good biocompatibility, mechanical flexibility, real-time monitoring, durability, and non-invasiveness (Souri et al., 2020). So far, many wearable strain sensors have been developed by incorporating advanced functional materials into stretchable support substrates (Choi et al., 2019). Recently, by combining traditional textile technology with electrical engineering, e-textile has become an attractive candidate for wearable sensors (Afroj et al., 2019; Hu et al., 2019; La et al., 2018; Wang et al., 2021; Zhao et al., 2019b). Specifically, fiber strain sensors, known as the convergence of strain sensing materials (conductive materials) and textile platforms, have been

[1]Research Center for Bioengineering and Sensing Technology, University of Science and Technology Beijing, Beijing 100083, P. R. China

[2]Guangdong Laboratory of Artificial Intelligence and Digital Economy (SZ), School of Biomedical Engineering, Shenzhen University Health Science Center, Shenzhen, Guangdong 518060, P. R. China

[3]Lead contact

*Correspondence: xutailin@ustb.edu.cn (T.X.)

*Correspondence .: zhangxueji@ustb.edu.cn (X.Z.)

https://doi.org/10.1016/j.isci.2020.102028

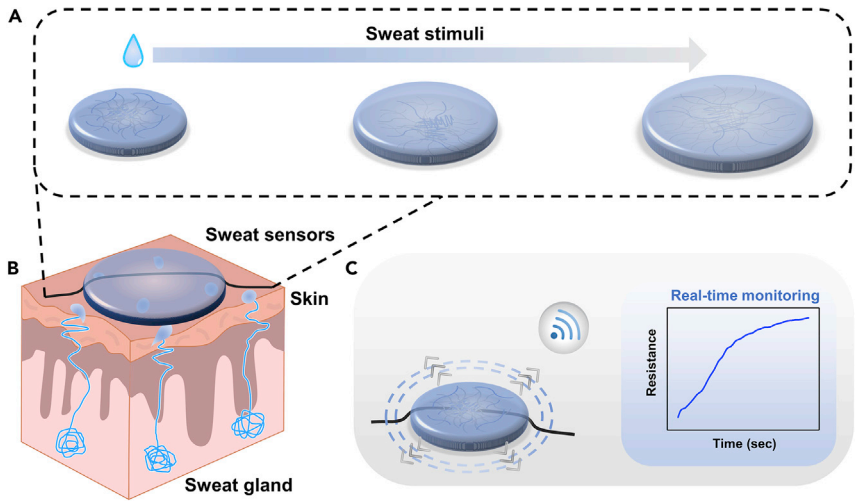

Figure 1. Design of wearable strain sensors for real-time sweat volume monitoring

(A) Schematic diagrams of super-absorbent hydrogel for sweat absorption, showing the swelling process of dry hydrogel (left) to the final equilibrium (right).

(B) Cross-section view of the structure of sweat glands, the wearable strain sensor has been placed across the skin's surface to wicking up the sweat.

(C) Schematic of the response of the swellable hydrogel induced strain sensing fabrics along with signal screening.

used to monitor various human activities (Gupta et al., 2018; Li et al., 2017; Liao et al., 2019; Yao et al., 2019).

Herein, we demonstrate the first example of wearable strain sensor for real-time sweat volume monitoring. Such approach employed the super-absorbent hydrogel (made by thermal cross-linking of polyacrylic acid (PAA)-polyvinyl alcohol (PVA) hydrogels) as absorbent materials to achieve sweat collection. The swelling of the hydrogel during sweat absorption caused the embedded strain sensing fabrics (fabricated by coating conductive carbon ink) to stretch and further led to the change of the resistance of the strain sensing fabric. Such sensor successfully converts sweat volume into intuitive changes in the resistivity of the strain sensing fabrics, and directly outputs the monitoring results through the computer. The hydrogels in this sensor can directly wick sweat up off the skin surface to swell, and then trigger the strain sensing fabrics response without any complicated fabrications or operations and any interference of motion or lighting. We designed the experiments to confirm that the sensor shows excellent repeatability, stability, and reliability (pH: 4–9 and salinity: 0–100 mM NaCl). Such simple to fabricate, low-cost sensor is able to continuously real-time monitor sweat volume, providing a novel measurement method of wearable sensors for monitoring sweat volume.

RESULTS AND DISCUSSION

Design of wearable strain sensors for real-time sweat volume monitoring

Figure 1 schematically demonstrates the workflow and the analytical strategy of wearable strain sensors for real-time sweat volume monitoring. The thread is directly dip-coated in conductive carbon ink to create a conductive layer on the surface of thread to obtain the strain sensing fabric. The super-absorbent hydrogel patch with strain sensing fabric inside is made by thermal cross-linking of PAA-PVA hydrogels (detailed fabrication processes are provided in the "Transparent Methods" section in the Supplemental Information). The super-absorbent hydrogels swell in their physical geometry along with the absorption of sweat as illustrated in Figure 1A. When the human body is triggered to sweat under heating or exercise conditions, wearable strain sensors combining super-absorbent hydrogel and strain sensing fabric can monitor sweat volume without any complicated operations (Figure 1B). Importantly, only the absorption of sweat can stimulate the hydrogel to swell and further stretch the embedded strain sensing fabrics when this sensor is on the body, inducing the resistance response of the strain-sensing fabric which can be directly recorded. Benefitting from the super-swelling property of hydrogel and strain sensitivity of carbon-coated thread, the sensor is able to continuously real-time monitor sweat volume by recording changes in the current signal as shown in Figure 1C.

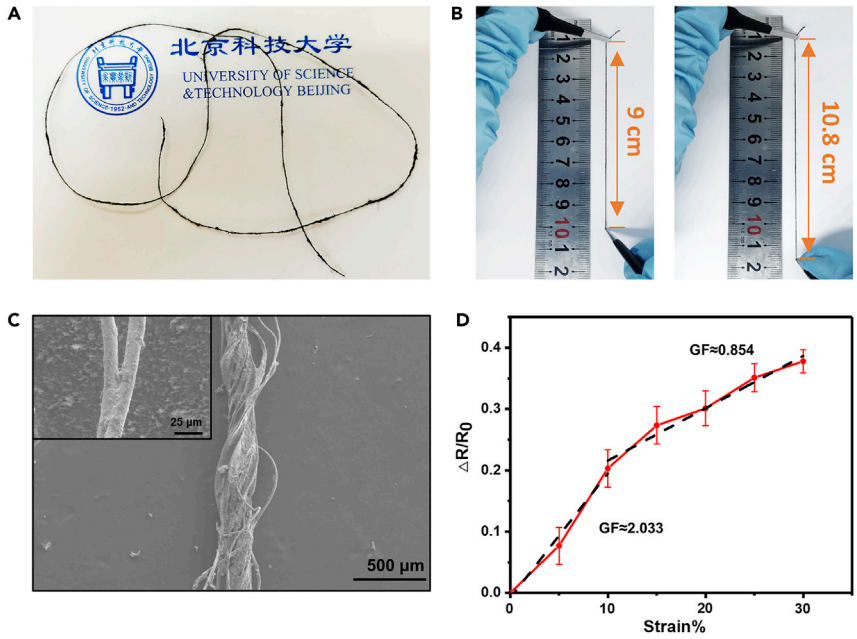

Figure 2. Characterization of strain sensing fabrics

(A) Photograph of the fabricated strain sensing fabrics.

(B) The stretchability of the strain sensing fabrics.

(C) The SEM images of the low-magnification and high-magnification strain sensing fabrics show a spiral structure and uniform coating. Scale bar: 500 μm and 25 μm respectively.

(D) Resistive response of strain sensing fabrics to strain. Data are presented as mean ± s.e.m. (n = 3).

Characterization of strain sensing fabrics

We characterized the strain sensing fabrics in details. Figure S1 presents a schematic illustration of the fabrication procedure of the strain sensing fabrics. The polybutylene terephthalate (PBT) stretchable puffy threads were harvested from a PBT bandage to fabricate the strain sensing fabrics. The fabrication of the strain sensing fabrics involved in two main steps: the thread is directly dip-coated in conductive carbon ink to create a conductive layer on the surface of thread and then cured in an atmospheric oven at 80°C for 30 min (Detail in Figure S1 and "Transparent Methods" Section). Figure 2A presents a photograph of the fabricated strain sensing fabrics, showing the change in the color of the thread due to the carbon dip-coating layer. The as-prepared strain sensing fabrics exhibit stretchability as shown in Figure 2B, which can be attributed to the helical and spiral shape of the thread's filaments. Figure 2C illustrates the SEM images of carbon-coated PBT thread in different magnification, in which the structure of the thread filaments twisted and entangled with each other is clearly observed. The typical SEM image of the strain sensing fabrics reveals that conductive carbon ink has been successfully coated on the surface of the PBT thread, and the average thickness of the conductive coating layer was ~3μm. The tensile force is various during the coating process, the thickness of the carbon coating at different parts will be slightly different, but this structural irregularity will not have a great impact on the performance of the strain sensing fabrics. Moreover, it can also be easily improved through automation. The relative change in the electrical resistance of the carbon-coated PBT strain sensing fabric is shown in Figure 2D with applied strain up to 30% of its initial length. The electrical resistance of the strain sensing fabrics is increasing with the strain applied, which resulted from the microcracks formation in the conductive carbon layer upon stretching. Correspondingly, the gauge factor (GF) of the strain sensing fabrics was evaluated as the slope of the graph in Figure 2D, which is defined as $GF = (|\Delta R|/R_0)/(\Delta L/L_0)$, where R_0, L_0 are the resistance and length before stretching, and ΔR, ΔL are the resistance and length changes before and after stretching. The strain sensing fabrics exhibited a GF of ~2.033 and ~0.854 for the strain range of 10% and 10–30%, respectively.

Optimization of the wearable strain sensor for real-time sweat volume monitoring

The position of the strain sensing fabrics relative to the hydrogel is important for monitoring sweat volume, and the sensors with different positions of the strain sensing fabrics have different perceptions and

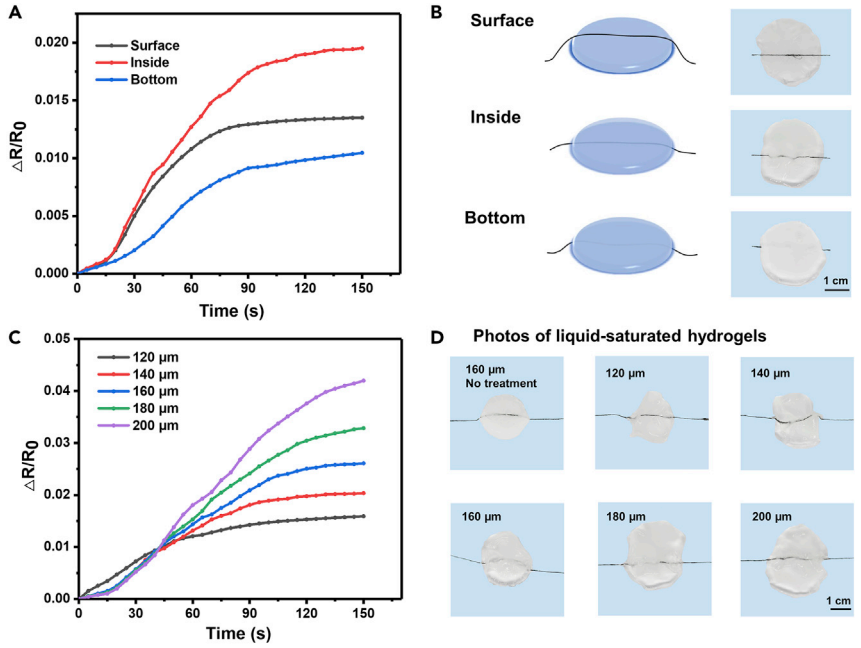

Figure 3. Optimization of the wearable strain sensor for real-time sweat volume monitoring

(A) The resistance response of the strain sensing fabric on the surface, inside and bottom of the hydrogel to sweat absorption.

(B) Illustration and photographs of placing the strain sensing fabrics on the surface, inside, and bottom of the hydrogel, respectively. Scale bar:1cm.

(C) The resistive response of sweat sensors with different initial dry hydrogel thicknesses against the fluid absorption.

(D) Photographs of liquid-saturated hydrogel sensors with different initial thickness. Scale bar:1cm.

responses to sweat absorption. Here, we compared the resistance response of placing the strain sensing fabrics on the surface, inside and bottom of the hydrogel to sweat absorption as displayed in Figures 3A and 3B. After attaching the strain sensing fabrics to the surface or bottom of the hydrogel patch, or placing it inside the hydrogel, 5 mL of 1 mM NaCl solution exceeding the fluid capacity of the hydrogel was added immediately to detect its resistance response. The results indicate that the strain sensing fabric inside the hydrogel is most sensitive to the sensing of the sweat absorption and swelling of the hydrogel, followed by the response of the strain sensing fabric on the surface of the hydrogel, and the least sensitive position is the bottom of the hydrogel (Figure 3A). Figure 3B exhibits the diagrams and photos of placing the strain sensing fabrics on the surface, inside, and bottom of the hydrogel, respectively. When the strain sensing fabric is inside the hydrogel, it is stretched by the swelling hydrogel, thereby more directly and sensitively sensing the geometric shape change of the hydrogel after sweat absorption. Therefore, for the rest of the experiments reported here, we have chosen to place the strain sensing fabric inside the hydrogel for sensing and monitoring.

Another important factor that affects sweat volume monitoring is the thickness of the swellable hydrogel. Thinner hydrogels may be more sensitive to the monitoring of smaller amounts of sweat, but if the hydrogel is too thin, the sensors could have limited detection range and the hydrogel could wrinkle during swelling and make the results unreliable. The thickness of the hydrogel was optimized to obtain the sweat sensors with excellent sensing performance and detection ability. Figure 3C demonstrates the resistive responses of sensors with different initial dry hydrogel thicknesses (120, 140, 160, 180 and 200 μm) after adding 5 mL of 1 mM NaCl solution exceeding the fluid capacity of the hydrogel to the sweat sensor. The results indicate that at the beginning, no significant difference in resistance response can be noticed between different thicknesses of sensors and after approximately 40 s, the thicker hydrogels tend to swell quickly leading to a rapid increase in the resistance response of the strain-sensing fabric. Eventually, as the hydrogel absorbs more and more solutions, the swelling force becomes weaker and weaker, and the resistance response of the strain sensing fabric also tends to be gentle. Figure 3D presents a photo of each sensor with different initial dry hydrogel thickness (120, 140, 160, 180, and 200μm) after 150 s of fluid absorption.

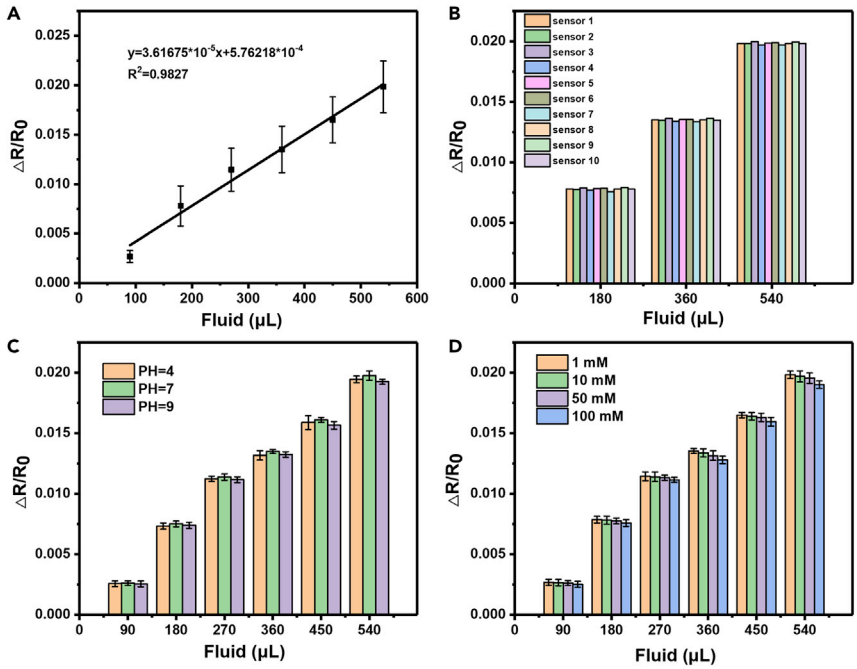

Figure 4. Measurement of the sweat volume *in vitro*

(A) Calibration curve of wearable strain sensor showing the resistance change of strain sensing fabrics vs. fluid volume added.

(B) The resistance response of 10 sweat volume monitoring sensors in 1 mM NaCl solution.

(C and D) The influence of various physiologically relevant pH (C) and salinity (D) on the performance of wearable strain sensor. Data are presented as mean ± s.e.m. (n = 3).

As expected, hydrogels of different thicknesses swelled, and geometric shapes expanded to varying degrees. Moreover, the thicker the material, the larger the geometric increase, and the higher the mechanical strength of the hydrogel sensor. Figure S2 displays a stepwise absorption-swelling process of a hydrogel sensor with an initial dry thickness of 160 μm, the hydrogels gradually expanded the volume, and at last was able to swell by 10–20× in volume in less than 3 min. Based on the results of Figures 3C and 3D, for the remaining experiments reported here, the initial dry thickness of the hydrogel sensor was 160μm.

Measurement of the sweat volume in vitro

We next characterized performances of the strain sensors to detect sweat volume. The sensors monitor sweat volume by measuring the resistance change of the strain sensing fabric inside the swellable hydrogel. Typically, the sweat rate range is considered to be 1–20 nL/min/gland and there are 150 sweat glands/cm^2 on the arm region (Sonner et al., 2015). In this case, total hydrogel sweat collection area is approximately 3 cm^2 and the injection rate of NaCl solution is around 9 μL/min. As shown in Figure 4A, the strain sensor could effectively detect the volumetric change of the fluid. The electrical resistance of the strain sensing fabric inside the swellable hydrogels increases as the hydrogel gradually swells when the NaCl solution was injected. And there is a linear relationship between the measured resistance response changes and the volume that the fluid injects. The addition of liquid directly converts the increased volume of the hydrogel, and it is further converted into the resistance signal of the strain sensing fabric. Therefore, from a measurement perspective, the linear response to the liquid volume is reasonable and attractive, and can be used for calibration. Additionally, the reproducibility of the sweat volume monitoring sensors was also studied by testing 10 sweat sensors in 1 mM NaCl solution, as displayed in Figure 4B. As expected, the sweat sensors have variation in resistance response at a definite fluid volume but with comparable behavior across all sensors. Meanwhile, we also explored the effect of relative humidity on the performance of the sweat sensor. As shown in Figure S3, the relative humidity has almost no effect on the performance of the sensor.

Additionally, we tested the sensor's performance in the non-pathological range for, sweat pH (4–9) (Diculescu et al., 2019) and salinity (1–100 mM NaCl) (Sempionatto et al., 2019) to evaluate the feasibility of the

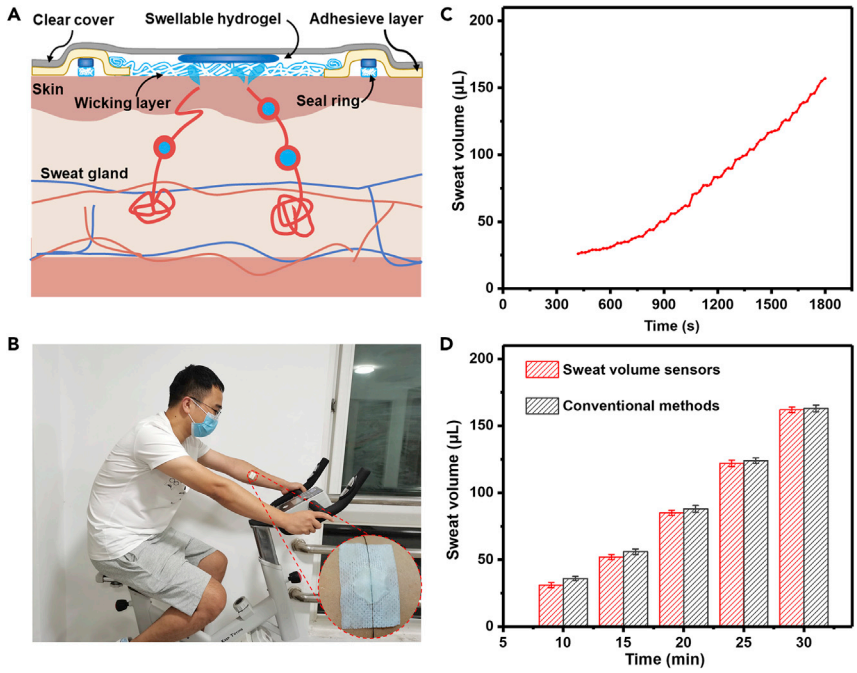

Figure 5. The design and results of the wearable strain sensor *in vivo*

(A) The complete design of the wearable strain sensor patch for the *in vivo* testing.

(B) The optical images of a subject wearing the wearable strain sensor patch on his forearms.

(C) On-body real-time measurements of sweat volume using the strain sensing patch.

(D) Comparison of sweat volume measurement from the strain sensing patch and conventional gravimetric analysis. Data are presented as mean ± s.e.m. (n = 3).

wearable strain sensor for real-time sweat volume monitoring for practical application. Figures 4C and 4D shows the response of the sensor in artificial sweat at various physiologically relevant pH and salinity. The sensors perform over a wide range of pH and salinity, fluid volume measurement remains relatively constant when pH and salinity change. Although the increased NaCl concentration tends to decrease the performance of the sensor, it only decreased significantly at the highest concentration in the physiological range (100 mM). Both pH and salinity in sweat have a wide range and change significantly with sweat volume. The data of Figures 4C and 4D confirms stable and repeatable performance of wearable strain sensor with varying pH and salinity.

The design and results of the wearable strain sensor in vivo

Finally, the wearable strain sensor was used for on-body analysis of sweat volume to demonstrate its feasibility for health monitoring applications. The complete design of the wearable strain sensor patch is illustrated in Figure 5A, which involves several additional features. Textiles as a wicking layer have excellent liquid absorption capability, collect, and deliver sweat from the skin to the hydrogel. Moreover, it also can effectively prevent the hydrogel patch with built-in strain sensing fabric from directly contacting the skin and being stretched. A seal ring is used to seal the sweat in a textile wicking layer on the skin surface to identify the sweat collection area and prevent sweat from entering outside the defined collection area.

As displayed in Figure 5B, participant wore patches on his forearms and performed stationary cycling for about 30 min. The detailed measurement protocol is included in the "Transparent Methods" section and Figure S4 in the Supplemental Information. Figure 5C shows the real-time measurement result of sweat volume on body using the wearable strain sensor patch. Here the measured sweat volume data conversion was done based on the calibration curve of Figure 4A as previously discussed. The result presents that sweat volume gradually increases as the exercise continues. Figure 5D shows the comparison of the sweat volume measurement results between the wearable strain sensor patch and the conventional gravimetric method. Among them, the data of conventional methods in Figure 5D are detected near the patch by classic

gravimetric analysis. The measurement of the sweat volume obtained from the patch we designed is basically consistent with that measured by traditional methods. The result shows that the proposed patch can be used for continuous sweat volume measurement and can be as reliable as gravimetric measurements.

Conclusion

In conclusion, we have demonstrated a wearable strain sensor for real-time sweat volume monitoring. To the best of our knowledge, this is the first example of the strain sensor used to monitor sweat volume. Such wearable strain sensors are realized via hydrogels directly wick sweat up off the skin surface to swell and then trigger the strain sensing fabrics response. Such sensor successfully converts sweat volume into intuitive changes in the resistivity of the strain sensing fabrics, and directly outputs the monitoring results through the computer. We have experimentally optimized the thickness of the swellable hydrogel and the position of the strain sensing fabric to improve sensors' performance. Compared to other methods and sensors (e.g. colorimetric method and microfluidic devices), our sweat sensing patches do not require complicated fabrications or operations and are not affected by motion or light. We also showed proof-of-concept analysis of preliminary *in vivo* testing of the strain sensor and demonstrated the capabilities of accurate measurement of sweat volume during physical activity. The sensor provides a novel measurement method of wearable devices for sweat volume monitoring and greatly expands the biosensing platform.

Limitations of the study

For wearable sensors, it is necessary to minimize the data reader as much as possible to achieve portability and practicality. In the future, it can be considered to integrate wireless communication electronics into the device. The transmission of wireless signals will bring great convenience to the use of the sensor. In addition, although we have designed the wicking layer, clear layer, etc. to protect the hydrogel sensor from external interference including human motion, further motion studies are still needed to quantify and confirm.

Resource availability

Lead contact

Further information and requests for resources and reagents should be directed to and will be fulfilled by the lead contact, Tailin Xu (xutailin@ustb.edu.cn).

Materials availability

This study did not generate new unique reagents.

Data and code availability

The published article includes all data generated or analyzed during this study.

METHODS

All methods can be found in the accompanying Transparent Methods supplemental file.

SUPPLEMENTAL INFORMATION

Supplemental Information can be found online at https://doi.org/10.1016/j.isci.2020.102028.

ACKNOWLEDGMENTS

We acknowledge funding from National Natural Science Foundation of China (21804007, 21890742), Beijing Natural Science Foundation (2184109), Fundamental Research Funds for Central Universities (FRF-TP-17-066A1), and National Postdoctoral Innovative Talents Support Program of China (BX20180036), China Postdoctoral Science Foundation (2019M650479).

AUTHOR CONTRIBUTIONS

W.L. and X. T. conceived and designed the experiments. W.L. and C.F. prepared materials, performed the experiments, and analyzed experimental data. W.L. wrote the manuscript. X. T. and Z.X. revised the manuscript, X. T. and Z.X. supervised all the aspects of this work and provided financial support. All authors discussed the results and contributed to the paper.

DECLARATION OF INTERESTS

The authors declare no competing interests.

Received: November 10, 2020
Revised: December 13, 2020
Accepted: December 29, 2020
Published: January 22, 2021

REFERENCES

Afroj, S., Karim, N., Wang, Z., Tan, S., He, P., Holwill, M., Ghazaryan, D., Fernando, A., and Novoselov, K.S. (2019). Engineering graphene flakes for wearable textile sensors via highly scalable and ultrafast yarn dyeing technique. ACS Nano *13*, 3847–3857.

Baker, L.B., Stofan, J.R., Lukaski, H.C., and Horswill, C.A. (2011). Exercise-induced trace mineral element concentration in regional versus whole-body wash-down sweat. Int. J. Sport Nutr. Exerc. Metab. *21*, 233–239.

Bandodkar, A.J., Gutruf, P., Choi, J., Lee, K., Sekine, Y., Reeder, J.T., Jeang, W.J., Aranyosi, A.J., Lee, S.P., Model, J.B., et al. (2019a). Battery-free, skin-interfaced microfluidic/electronic systems for simultaneous electrochemical, colorimetric, and volumetric analysis of sweat. Sci. Adv. *5*, eaav3294.

Bandodkar, A.J., Jeang, W.J., Ghaffari, R., and Rogers, J.A. (2019b). Wearable sensors for Biochemical sweat analysis. Annu. Rev. Anal. Chem. *12*, 1–22.

Bariya, M., Nyein, H.Y.Y., and Javey, A. (2018). Wearable sweat sensors. Nat. Electron. *1*, 160–171.

Brothers, M.C., DeBrosse, M., Grigsby, C.C., Naik, R.R., Hussain, S.M., Heikenfeld, J., and Kim, S.S. (2019). Achievements and challenges for real-time sensing of analytes in sweat within wearable platforms. Acc. Chem. Res. *52*, 297–306.

Choi, J., Ghaffari, R., Baker, L.B., and Rogers, J.A. (2018). Skin-interfaced systems for sweat collection and analytics. Sci. Adv. *4*, eaar3921.

Choi, S., Han, S.I., Kim, D., Hyeon, T., and Kim, D.H. (2019). High-performance stretchable conductive nanocomposites: materials, processes, and device applications. Chem. Soc. Rev. *48*, 1566–1595.

Diculescu, V.C., Beregoi, M., Evanghelidis, A., Negrea, R.F., Apostol, N.G., and Enculescu, I. (2019). Palladium/palladium oxide coated electrospun fibers for wearable sweat pH-sensors. Sci. Rep. *9*, 8902.

Francis, J., Stamper, I., Heikenfeld, J., and Gomez, E.F. (2018). Digital nanoliter to milliliter flow rate sensor with in vivo demonstration for continuous sweat rate measurement. Lab Chip *19*, 178–185.

Gao, W., Emaminejad, S., Nyein, H.Y.Y., Challa, S., Chen, K., Peck, A., Fahad, H.M., Ota, H., Shiraki, H., Kiriya, D., et al. (2016). Fully integrated wearable sensor arrays for multiplexed in situ perspiration analysis. Nature *529*, 509–514.

Gupta, N., Rao, K.D.M., Srivastava, K., Gupta, R., Kumar, A., Marconnet, A., Fisher, T.S., and Kulkarni, G.U. (2018). Cosmetically adaptable transparent strain sensor for sensitively delineating patterns in small movements of vital human organs. ACS Appl. Mater. Inter. *10*, 44126–44133.

He, X., Xu, T., Gu, Z., Gao, W., Xu, L.P., Pan, T., and Zhang, X. (2019). Flexible and superwettable bands as a platform toward sweat sampling and sensing. Anal. Chem. *91*, 4296–4300.

He, X., Yang, S., Pei, Q., Song, Y., Liu, C., Xu, T., and Zhang, X. (2020). Integrated smart janus textile bands for self-pumping sweat sampling and analysis. ACS Sens. *5*, 1548–1554.

Heikenfeld, J. (2016). Non-invasive analyte access and sensing through eccrine sweat: challenges and outlook circa 2016. Electroanalysis *28*, 1242–1249.

Hines, L., Petersen, K., Lum, G.Z., and Sitti, M. (2017). Soft actuators for small-scale robotics. Adv. Mater. *29*, 1603483.

Hu, X., Tian, M., Xu, T., Sun, X., Sun, B., Sun, C., Liu, X., Zhang, X., and Qu, L. (2019). Multiscale disordered porous fibers for self-sensing and self-cooling integrated smart sportswear. ACS Nano *14*, 559–567.

Hua, Q., Sun, J., Liu, H., Bao, R., Yu, R., Zhai, J., Pan, C., and Wang, Z.L. (2018). Skin-inspired highly stretchable and conformable matrix networks for multifunctional sensing. Nat. Commun. *9*, 244.

Kang, D., Pikhitsa, P.V., Choi, Y.W., Lee, C., Shin, S.S., Piao, L., Park, B., Suh, K.Y., Kim, T.I., and Choi, M. (2014). Ultrasensitive mechanical crack-based sensor inspired by the spider sensory system. Nature *516*, 222–226.

Kang, T.H., Chang, H., Choi, D., Kim, S., Moon, J., Lim, J.A., Lee, K.Y., and Yi, H. (2019). Hydrogel-templated transfer-printing of conductive nanonetworks for wearable sensors on topographic flexible substrates. Nano Lett. *19*, 3684–3691.

Kaya, T., Liu, G., Ho, J., Yelamarthi, K., Miller, K., Edwards, J., and Stannard, A. (2019). Wearable sweat sensors: background and current trends. Electroanalysis *31*, 411–421.

Kim, G., Cho, S., Chang, K., Kim, W.S., Kang, H., Ryu, S.P., Myoung, J., Park, J., Park, C., and Shim, W. (2017). Spatially pressure-mapped thermochromic interactive sensor. Adv. Mater. *29*, 1606120.

Kim, J., Campbell, A.S., de Avila, B.E., and Wang, J. (2019). Wearable biosensors for healthcare monitoring. Nat. Biotechnol. *37*, 389–406.

Kim, J., Lee, M., Shim, H.J., Ghaffari, R., Cho, H.R., Son, D., Jung, Y.H., Soh, M., Choi, C., Jung, S., et al. (2014). Stretchable silicon nanoribbon electronics for skin prosthesis. Nat. Commun. *5*, 5747.

Kim, S.B., Lee, K., Raj, M.S., Lee, B., Reeder, J.T., Koo, J., Hourlier-Fargette, A., Bandodkar, A.J., Won, S.M., Sekine, Y., et al. (2018). Soft, skin-interfaced microfluidic systems with wireless, battery-Free electronics for digital, real-time tracking of sweat loss and electrolyte composition. Small *14*, e1802876.

Koh, A., Kang, D., Xue, Y., Lee, S., Pielak, R.M., Kim, J., Hwang, T., Min, S., Banks, A., Bastien, P., et al. (2016). A soft, wearable microfluidic device for the capture, storage, and colorimetric sensing of sweat. Sci. Transl. Med. *8*, 366ra165.

La, T.G., Qiu, S., Scott, D.K., Bakhtiari, R., Kuziek, J.W.P., Mathewson, K.E., Rieger, J., and Chung, H.J. (2018). Two-layered and stretchable e-textile patches for wearable healthcare electronics. Adv. Healthc. Mater. *7*, e1801033.

Li, Y., Li, Y., Su, M., Li, W., Li, Y., Li, H., Qian, X., Zhang, X., Li, F., and Song, Y. (2017). Electronic textile by dyeing method for multiresolution physical kineses monitoring. Adv. Electron. Mater. *3*, 1700253.

Liao, X., Wang, W., Wang, L., Tang, K., and Zheng, Y. (2019). Controllably enhancing stretchability of highly sensitive fiber-based strain sensors for intelligent monitoring. ACS Appl. Mater. Inter. *11*, 2431–2440.

Lim, S., Son, D., Kim, J., Lee, Y.B., Song, J.-K., Choi, S., Lee, D.J., Kim, J.H., Lee, M., Hyeon, T., et al. (2015). Transparent and stretchable interactive human machine interface based on patterned graphene heterostructures. Adv. Funct. Mater. *25*, 375–383.

Liu, C., Xu, T., Wang, D., and Zhang, X. (2020). The role of sampling in wearable sweat sensors. Talanta *212*, 120801.

Liu, Y.J., Cao, W.T., Ma, M.G., and Wan, P. (2017). Ultrasensitive wearable soft strain sensors of conductive, self-healing, and elastic hydrogels with synergistic "soft and hard" hybrid networks. ACS Appl. Mater. Inter. *9*, 25559–25570.

Nyein, H.Y.Y., Bariya, M., Kivimäki, L., Uusitalo, S., Liaw, T.S., Jansson, E., Ahn, C.H., Hangasky, J.A., Zhao, J., Lin, Y., et al. (2019). Regional and correlative sweat analysis using high-throughput microfluidic sensing patches toward decoding sweat. Sci. Adv. *5*, eaaw9906.

Nyein, H.Y.Y., Tai, L.C., Ngo, Q.P., Chao, M., Zhang, G.B., Gao, W., Bariya, M., Bullock, J., Kim, H., Fahad, H.M., et al. (2018). A wearable microfluidic sensing patch for dynamic sweat secretion analysis. ACS Sens. *3*, 944–952.

Park, S., Kim, H., Vosgueritchian, M., Cheon, S., Kim, H., Koo, J.H., Kim, T.R., Lee, S., Schwartz, G., Chang, H., et al. (2014). Stretchable energy-harvesting tactile electronic skin capable of differentiating multiple mechanical stimuli modes. Adv. Mater. *26*, 7324–7332.

Ray, T.R., Choi, J., Bandodkar, A.J., Krishnan, S., Gutruf, P., Tian, L., Ghaffari, R., and Rogers, J.A. (2019). Bio-Integrated wearable systems: a comprehensive review. Chem. Rev. *119*, 5461–5533.

Sempionatto, J.R., Martin, A., García-Carmona, L., Barfidokht, A., Kurniawan, J.F., Moreto, J.R., Tang, G., Shin, A., Liu, X., Escarpa, A., et al. (2019). Skin-worn soft microfluidic potentiometric detection system. Electroanalysis *31*, 239–245.

Sonner, Z., Wilder, E., Heikenfeld, J., Kasting, G., Beyette, F., Swaile, D., Sherman, F., Joyce, J., Hagen, J., Kelley-Loughnane, N., et al. (2015). The microfluidics of the eccrine sweat gland, including biomarker partitioning, transport, and biosensing implications. Biomicrofluidics *9*, 031301.

Souri, H., Banerjee, H., Jusufi, A., Radacsi, N., Stokes, A.A., Park, I., Sitti, M., and Amjadi, M. (2020). Wearable and stretchable strain sensors: materials, sensing mechanisms, and applications. Adv. Intell. Syst. *2*, 2000039.

Tee1, B.C.-K., Chortos, A., Berndt, A., Nguyen, A.K., Tom, A., McGuire, A., Lin, Z.C., Tien, K., Bae, W.-G., Wang, H., et al. (2015). A skin-inspired organic digital mechanoreceptor. Science *350*, 313–316.

Tian, G., Xiong, D., Su, Y., Yang, T., Gao, Y., Yan, C., Deng, W., Jin, L., Zhang, H., Fan, X., et al. (2020). Understanding the potential screening effect through the discretely structured ZnO nanorods piezo array. Nano Lett. *20*, 4270–4277.

Trung, T.Q., and Lee, N.E. (2016). Flexible and stretchable physical sensor integrated platforms for wearable human-activity monitoring and personal healthcare. Adv. Mater. *28*, 4338–4372.

Wang, R., Zhai, Q., An, T., Gong, S., and Cheng, W. (2021). Stretchable gold fiber-based wearable textile electrochemical biosensor for lactate monitoring in sweat. Talanta *222*, 121484.

Wang, X., Liu, Z., and Zhang, T. (2017). Flexible sensing electronics for wearable/attachable health monitoring. Small *13*, 1602790.

Yang, T., Pan, H., Tian, G., Zhang, B., Xiong, D., Gao, Y., Yan, C., Chu, X., Chen, N., Zhong, S., et al. (2020). Hierarchically structured PVDF/ZnO core-shell nanofibers for self-powered physiological monitoring electronics. Nano Energy *72*, 104706.

Yang, Y., and Gao, W. (2019). Wearable and flexible electronics for continuous molecular monitoring. Chem. Soc. Rev. *48*, 1465–1491.

Yang, Y., Song, Y., Bo, X., Min, J., Pak, O.S., Zhu, L., Wang, M., Tu, J., Kogan, A., Zhang, H., et al. (2019). A laser-engraved wearable sensor for sensitive detection of uric acid and tyrosine in sweat. Nat. Biotechnol. *38*, 217–224.

Yao, S., Yang, J., Poblete, F.R., Hu, X., and Zhu, Y. (2019). Multifunctional electronic textiles using silver nanowire composites. ACS Appl. Mater. Inter. *11*, 31028–31037.

Yuan, Z., Hou, L., Bariya, M., Nyein, H.Y.Y., Tai, L.C., Ji, W., Li, L., and Javey, A. (2019). A multi-modal sweat sensing patch for cross-verification of sweat rate, total ionic charge, and Na(+) concentration. Lab Chip *19*, 3179–3189.

Zhang, B., Zhang, L., Deng, W., Jin, L., Chun, F., Pan, H., Gu, B., Zhang, H., Lv, Z., Yang, W., et al. (2017a). Self-powered acceleration sensor based on liquid metal triboelectric nanogenerator for vibration monitoring. ACS Nano *11*, 7440–7446.

Zhang, S.L., Lai, Y.-C., He, X., Liu, R., Zi, Y., and Wang, Z.L. (2017b). Auxetic foam-based contact-mode triboelectric nanogenerator with highly sensitive self-powered strain sensing capabilities to monitor human body movement. Adv. Funct. Mater. *27*, 1606695.

Zhao, F.J., Bonmarin, M., Chen, Z.C., Larson, M., Fay, D., Runnoe, D., and Heikenfeld, J. (2019a). Ultra-simple wearable local sweat volume monitoring patch based on swellable hydrogels. Lab Chip *20*, 168–174.

Zhao, Y., Zhai, Q., Dong, D., An, T., Gong, S., Shi, Q., and Cheng, W. (2019b). Highly stretchable and strain-insensitive fiber-based wearable electrochemical biosensor to monitor glucose in the sweat. Anal. Chem. *91*, 6569–6576.

iScience, Volume *24*

Supplemental Information

Wearable strain sensor for real-time sweat volume monitoring

Lirong Wang, Tailin Xu, Chuan Fan, and Xueji Zhang

Supplemental Figures

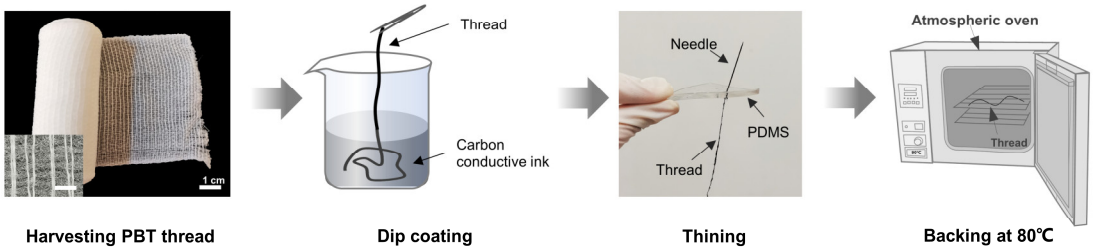

Figure S1. Schematic of the fabrication process of strain sensing fabrics by dip coating the thread directly in carbon conductive ink, Related to Figure 2. The scale bar for magnified picture of the PBT band is 1mm.

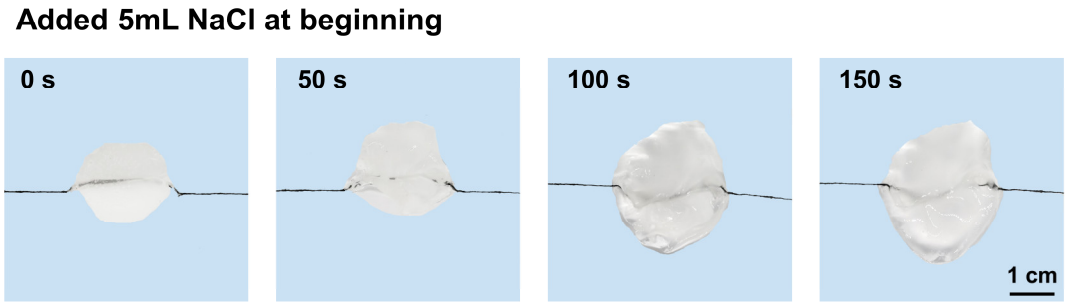

Figure S2. The pictures of the swelling process of initial dry hydrogel with a thickness of 160 μm in 150s, Related to Figure 3.

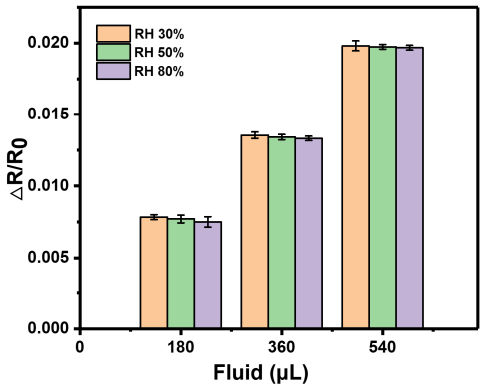

Figure S3. The influence of various relative humidity on the performance of wearable strain sensor, Related to Figure 4. Data are presented as mean ± s.e.m. (n = 3).

Figure S4. The process of the wearable strain sensor patch in vivo testing, Related to Figure 5.

Transparent Methods

Materials and instruments

Poly (vinyl alcohol) (PVA, ~98% hydrolyzed, DP = 1750 ± 50), Sodium polyacrylate were collected from Aladdin, Shanghai, China. Polybutylene terephthalate (PBT) bandage were bought from Tutai (Shanghai, China) Conductive carbon ink (YH-601CA) was obtained from Capiton (Shenzhen, China). The poly tetra fluoroethylene (PTFE) model was customized by HuaQiang Seiko (Shenzhen, China). A field-emission scanning electron microscope (SEM, JSM-6700F, Japan) was used for characterizing the morphologies of carbon-coated PBT thread. A Longer TS-1A syringe pump was used to control the fluid flow rate. A digital source-meter (Keithley 2400-SMU) and a standard digital multimeter (UNIT UT39C) were used to detect and record the electrical

signals of the strain sensing fabrics. All the optical photography was captured by a mobile phone.

Fabrication of the super absorbent hydrogel

The super absorbent hydrogel was made by thermal cross-linking of sodium polyacrylate hydrogels with poly (vinyl alcohol) hydrogels (PAA-PVA hydrogels). 10 g of sodium polyacrylate was added to 400 mL of water and stirred at 60 ° C for 1 hour. And then 10% of polyvinyl alcohol was added. After mixing well, the mixture was coated on a Teflon model and dried at 40 °C overnight. The resulting hydrogel film was finally dried with a desiccant to prevent water absorption during storage.

Fabrication of the strain sensing fabrics

Briefly, the strain sensing fabrics were fabricated by coating a carbon-resistant ink on the puffy thread of polybutylene terephthalate (PBT)(Sadeqi et al., 2018). As shown in **Figure S1**, the PBT puffy threads were harvested from a PBT bandage firstly. Next, the thread was dipped in a carbon-resistant ink to form a conductive layer on the thread. In order to make the coating uniform and further thinner, a needle was used to pass the thread through a 5 mm thick cured polydimethylsiloxane (PDMS) film. Finally, the coating thread was cured in an atmospheric oven at 80 ° C for 30 minutes.

In vitro testing of the sweat sensing hydrogel patch

The prepared strain sensing fabric was attached to the top or bottom surface of the hydrogel film,

or putted it inside the hydrogel to prepare a complete hydrogel sensor patch. At room temperature 25℃and RH30%, the hydrogel patch combined with strain sensing fabric was placed in a plate, and both ends of the strain sensing fabric were connected to a digital source meter (Keithley 2400 SourceMeter) through wires to monitor the resistance change. A syringe pump (Longer TS-1A) next to the hydrogel patch was used to apply fluid and control the flow rate. The photographs of the hydrogel patch combined with strain sensing fabric were taken by a mobile phone.

In vivo testing of the sweat sensing hydrogel patch

The experiment protocols were strictly guided by Animal and Human Experimentation Committee of University of Science and Technology Beijing (USTB). A 30-year-old healthy male volunteer was recruited from USTB and gave written informed consent before testing. Before placing the sweat sensor hydrogel patch, the subject's forearm was wiped and cleaned with alcohol swabs and gauze for in-situ detection. The sweat sensor hydrogel patch was placed on the arm, and the two ends of the strain sensing fabric built into the hydrogel patch were connected to a DC source meter (Keithley 2400 SourceMeter). Then the subject was required to exercise continuously for about 30 minutes, during which the sweat volume was measured by the sensor and directly transmitted the data to the computer through Keithley 2400 SourceMeter. Finally, the computer uses the standard curve to convert the resistance change into the sweat volume and output the result. The traditional perspiration detection method uses gravimetric analysis, that is, dry gauze is used to wipe off the sweat of the same area near the patch every 5 minutes, and the weight difference is weighed to calculate the perspiration.

Supplemental References

Sadeqi, A., Nejad, H.R., Alaimo, F., Yun, H., Punjiya, M., and Sonkusale, S. (2018). Washable Smart Threads for Strain Sensing Fabrics. IEEE Sens J, 9137-9144.